

## An oscillating bottom boundary layer connects the littoral and pelagic regions of Lake Opeongo, Canada

Melissa Anne Coman and Mathew Graeme Wells

### ABSTRACT

The movement of a thermocline can drive strong benthic currents, which can transport nutrients from sediments into the water column via pore water advection or sediment resuspension. We report field observations of near-shore benthic velocities and offshore thermocline movements in Lake Opeongo; a medium-sized lake typical of the Canadian Shield. We find that during large thermocline deflections there are sustained currents  $>6 \text{ cm s}^{-1}$  in the near-shore benthic layer. The mean current was  $1.75 \text{ cm s}^{-1}$  and the maximum current is  $10.3 \text{ cm s}^{-1}$ . At our site, the net transport is offshore even though the thermocline oscillates up and down so that currents are sometimes upslope and inshore. We estimate the excursion length of a water parcel over the 31-day deployment period, and determine that the mean daily excursion length is 630 m, with the maximum value being 2 km offshore. Given that the south arm of Lake Opeongo is 6 km long and 0.6 km wide, the predicted excursion length of water implies that there is strong connectivity between the sediment in the littoral zone, and the metalimnetic waters offshore. As Lake Opeongo is oligotrophic, any nutrient pulses from the sediment will be quickly taken up by the plankton.

**Key words** | basin scale seiche, benthic currents, nutrient transport, offshore transport

Melissa Anne Coman  
Mathew Graeme Wells (corresponding author)  
Department of Physical and Environmental  
Sciences,  
University of Toronto Scarborough,  
1265 Military Trail,  
Toronto, ON,  
Canada M1C 1A4  
E-mail: wells@utsc.utoronto.ca

### INTRODUCTION

It is important to understand the exchange of water and dissolved nutrients between the benthic and pelagic zones of a lake so that food web dynamics can be correctly modelled. One mechanism of nutrient addition to the water column originates from pore water advection into the benthic water (Kirillin *et al.* 2009). Pore water is the interstitial fluid in the lake sediment and therefore has a high concentration of nutrients (e.g. nitrogen and phosphorus). Pore water is advected into the benthic water via a suction action driven by strong benthic currents (Søndergaard *et al.* 2001; Kirillin *et al.* 2009; Basterretxea *et al.* 2011) or through direct resuspension of sediments (Gloor *et al.* 1994). A slower, but continuous, process that also adds nutrients into the water column is diffusion across the nutrient gradient which exists between the sediments and the water column (Levine & Schindler 1992; Sundbäck *et al.* 2003). The fate of any pore water that has been moved into the benthic region relies on the water circulation of the lake.

Bottom turbulence will enable pore water to be mixed into the bottom boundary layer of the lake and subsequent transport of this fluid into the pelagic zone will make the nutrients available to a wider range of organisms. Absence of a mechanism to mix the pore water into the boundary layer or lack of transport into the pelagic zone will severely limit the usefulness of any nutrients contained in the pore water. Therefore, a good understanding of the ability of boundary layer fluid to be transported into various regions of a lake will be essential in understanding this pathway of nutrient addition to a lake's food web.

The circulation of water in Lake Opeongo is dominated by wind-driven seiche events (Coman & Wells 2012). For a lake or reservoir with a fairly uniform cross section, surface wind forcing will set up a horizontal pressure gradient along the lake axis aligned with the wind direction. If the lake is stratified with a strong thermocline (as many medium-sized Canadian Shield lakes are during summer

time), this pressure gradient is balanced by a tilting of the thermocline. In this case, the thermocline is pushed downwards at the downwind end of the basin, and is pushed upwards at the upwind end of the basin as shown in Figure 1(a). The cessation or reduction of this wind forcing reduces the strength of the horizontal pressure gradient and releases the thermocline from the tilted orientation so that it relaxes back to its equilibrium level, shown in Figure 1(b). During this process the surface wind forcing has added momentum to the lake system so that upon wind reduction the thermocline does not simply return to its equilibrium level but undergoes seiching (shown in Figures 1(c) and 1(d)) until all the energy injected by the wind forcing has dissipated, or until another wind-forcing event re-establishes a new thermocline tilt. This oscillation is the basin scale seiche and is the major response of

surface wind forcing in Lake Opeongo (Coman & Wells 2012) and other lakes. The deflected thermocline extends to the lake boundaries, and the movements associated with seiching cause currents along the benthic inshore regions. When the thermocline is upwelling, the current direction along the slope will be upslope and when the thermocline is downwelling the current direction will be downslope in the inshore benthic region. When an inshore site is experiencing an upwelling, the local water temperature will be decreasing as hypolimnetic water moves up the slope. Similarly, during a downwelling, the site experiences warming temperatures as the hypolimnetic water departs and is replaced with epilimnion water, as shown in Figure 1(e). Therefore, under this simple representation of the consequences of surface wind forcing on medium-sized lakes, we expect downslope currents and warming

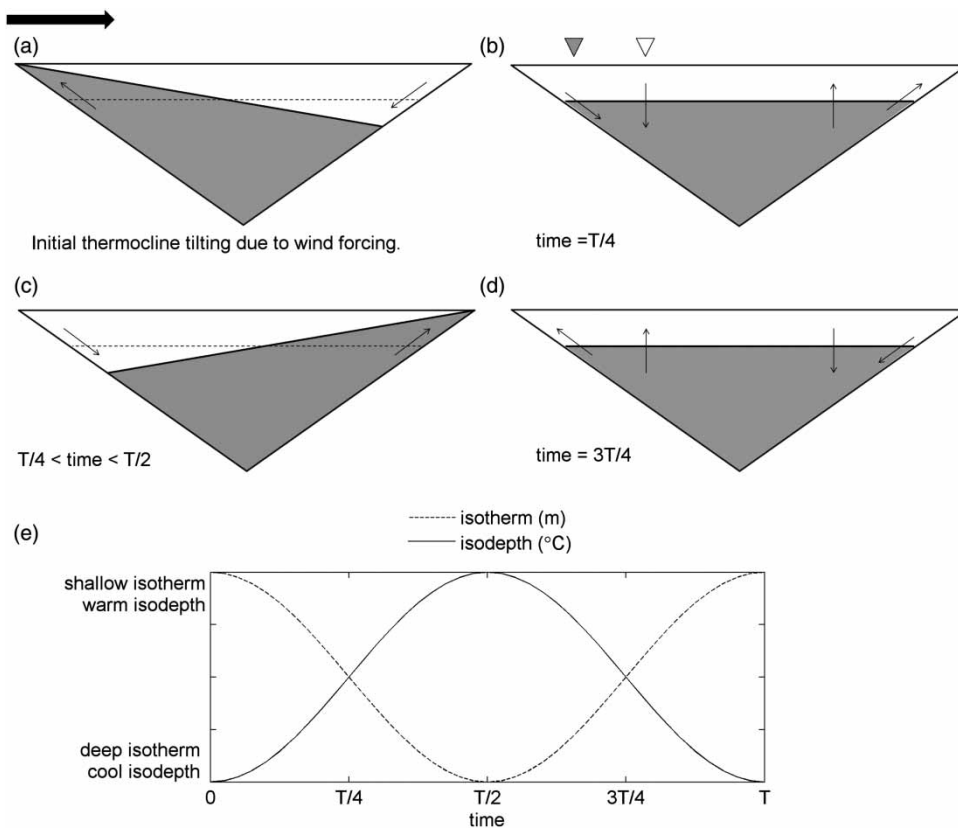


**Figure 1** | Schematic of thermocline tilting and inshore current direction. The solid line represents a thermocline, and the direction of currents and water movements are shown by arrows. Solid triangle represents relative inshore site location and open triangle represents relative offshore site location. Time is shown as a fraction of the basin scale seiche period,  $T$ . (a) The wind forcing has deflected the thermocline so that there is upwelling at the upwind end. (b) After the wind ceases the thermocline returns to its level of neutral buoyancy. (c) The thermocline then continues to oscillate such that maximum downwelling occurs at the original upwind end (time =  $T/2$ ) after which the currents again reverse and in (d) the thermocline is again at equilibrium level. One seiche cycle is complete if upwelling occurs again at the upwind end of the basin when time =  $T$ . (e) The relative depth of the offshore isotherm and the relative temperature at a fixed depth at the inshore site.

temperature in the inshore region during a downwelling event and upslope currents and cooling temperature during an upwelling event (Figure 1(e)). In addition, if we measure isotherms at a more offshore location we expect the motion of these isotherms to be consistent with those inshore. That is, an upwelling event is caused by a deflected thermocline so this motion will be evident in the isotherm record of an offshore site (as long as the offshore site is not in the centre of the thermocline's tilting axis). If the offshore site is between the centre point of the lake wind axis and the inshore site (open triangle in Figure 1(b)) then an upwelling event will be preceded by isotherms that decrease in depth and a downwelling event will be preceded by offshore isotherms that move deeper into the lake.

In Lake Opeongo, the basin scale seiche is forced by westerly winds, and has a period of about 12 hours. Coman & Wells (2012) found that the maximum displacement of the thermocline due to these motions has a strong dependence on surface wind forcing, lake stratification and basin morphometry. The largest displacement they measured was 10.7 m while the mean value was just 1.4 m. With a slope at the inshore site of 1%, these values imply a washing zone length of 1 km for the maximum thermocline displacement and a length of 140 m for mean displacement.

The magnitude of the thermocline tilt can be parameterised in terms of Lake number. The Lake number is a dimensionless parameter that combines the wind forcing and lake stratification, as well as including a measure of basin morphometry. Field observations in Lake Opeongo by Coman & Wells (2012) found that the maximum displacement of the thermocline is proportional to the inverse of the Lake number. This result will apply to any lake with a strong and sharp thermocline (i.e. thickness of thermocline is less than the epilimnion or hypolimnion thickness) and a triangular basin morphometry. This relationship was initially partially confirmed by Stevens & Lawrence (1997) who measured the Wedderburn number and thermocline deflection in four different sized Canadian lakes.

The magnitude of benthic turbulence in a stratified lake is also related to the magnitude of the seiching and hence the Lake number. For instance MacIntyre *et al.* (1999) found enhanced boundary mixing following low Lake number events in Mono Lake. Coman & Wells (2012) also found that low values of the Lake number are associated

with occurrences of temperature inversions in the near-shore benthic region. In Lake Opeongo, Coman & Wells (2012) also found that the slope of the benthos played a role in the amount of temperature inversions measured at near-shore sites, most likely due to breaking of high frequency internal waves generated on the internal seiche (Michallet & Ivey 1999; Horn *et al.* 2001). Hence after a strong wind event the most turbulent benthic regions of a lake are expected to be those with lower slope angles that are located near the depth of the thermocline. These shallow slopes will also be the benthic regions that have the greatest temperature variability.

There are many observations of large-scale internal seiches in lakes (Lorke 2007; Wells & Parker 2010). Resuspension of bottom sediments due to lake seiches has been directly observed (Shteinman *et al.* 1997) by tracking marked particles in the bed of Lake Kinneret, resulting in resuspended phosphates which enhanced the algal productivity in the water column (Ostrovsky *et al.* 1996). Indirect observations of particle resuspension due to large amplitude lake seiches include observations of elevated suspended particle concentrations near the lakebed (Gloor *et al.* 1994; Hawley & Muzzi 2003) and observations of increased phosphate fluxes after strong seiche events (MacIntyre *et al.* 1999). The resuspended phosphates arising from benthic turbulence may either be used locally or may be taken offshore by horizontal intrusions (Wain & Rehmann 2010) formed on the sloping boundaries of the lake.

Several field experiments have documented the role of benthic turbulence in driving intrusions away from a sloping boundary. Inall (2009) conducted the first field experiment that measured the fate of dye injected just above the sloping boundary layer in a long fjord where boundary mixing occurs via the interaction between the semidiurnal tide and rough topography. The dye initially spread in the vertical, a portion entered the boundary layer and subsequently intruded into the interior of the fjord in three distinct layers. The intrusions were driven by the gravitational collapse of the mixed boundary layer fluid and subsequent intrusion along isopycnal surfaces. The experiments of Wain & Rehmann (2010) tracked an intrusion from dye injected directly into the turbulent boundary layer on a sloping boundary (5–10%) into the interior of a lake. Their study

was conducted in a small lake with a fetch in primary wind direction of 700 m. Energised boundary mixing was driven by an internal seiche in response to a strong wind event. Rhodamine dye was injected into the boundary layer to act as a tracer and subsequent dye concentration mapping measured the three-dimensional (3D) extent of the tracer. After 1 day the intrusion generated by boundary mixing was 0.5–1 m thick and reached over 200 m offshore.

Transport from the sloping boundary to the interior may also occur due to asymmetries in the benthic flow field as the thermocline moves up and down the lakebed. Nakayama & Imberger (2010) showed that due to details of the stratified turbulence on a sloping boundary there would be a net offshore transport. In a lake there may also be a basin scale circulation set up by wind-driven forcing, whereby on average water is drawn in at the edges of the lake and exits in the central axis of the lake, similar to the wind-driven double gyre circulation pattern described in Rao & Murty (1970).

In this paper we will quantify the benthic currents that are driven by oscillations in the position of the thermocline. Our study takes place in the same region of Lake Opeongo as described by Coman & Wells (2012) and extends this study with new observations of the benthic currents measured with a downwards facing acoustic Doppler profiler. The main focus of the paper is to relate the observations of benthic currents and changes in water temperature to the occurrence of seiching motions in the lake. Specifically,

we show that oscillating currents lead to a net transport of water from the shallow littoral zone to the offshore pelagic zone.

## METHODS

The research presented here was conducted in Lake Opeongo, Algonquin Provincial Park, Ontario, Canada (Figure 2) between 15 July and 15 August 2010. Lake Opeongo is a low nutrient, medium-sized lake typical of many Canadian Shield lakes. Lake Opeongo contains four basins with a total surface area of 58.6 km<sup>2</sup>. We instrumented the South Arm basin which is roughly orientated in an east–west direction with a maximum fetch of 7.2 km, a surface area of 22.1 km<sup>2</sup>, an average depth of 14.6 m, and a maximum depth of 51.8 m (King *et al.* 1999; Finlay *et al.* 2001). In 2010 the lake was stratified for the entire deployment period with the thermocline at a depth of 7 m in the middle of July and deepening smoothly to 9 m by the middle of August. The depth of the thermocline was defined as the region with the maximum temperature gradient using the metrics in Read *et al.* (2011). A weather station was mounted on a very small island in the South Arm of Lake Opeongo (78°23.5' W, 45°42' N). It was operational for the last 10 days of our deployment. These data and previous year's weather data (Coman & Wells 2012) show that the wind blows predominately from the west and that there is

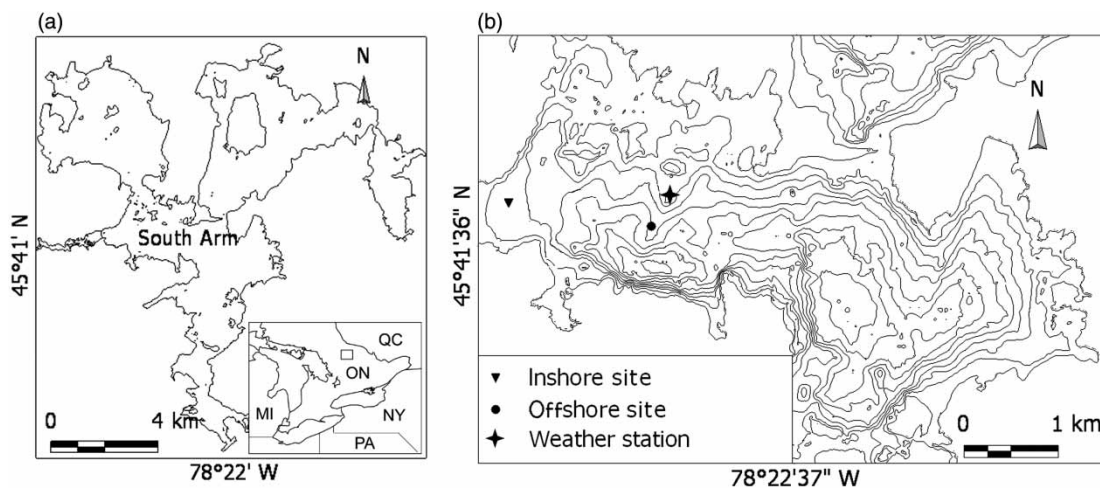


**Figure 2** | Map of (a) Lake Opeongo, and (b) the South Arm of Lake Opeongo with the inshore and offshore sites indicated with a triangle and circle, respectively, and the weather station shown by the star. The contour interval is 5 m.

typically a strong diurnal cycle in the winds, with peak winds occurring in mid afternoon. The offshore site was instrumented with a chain of thermistors (Onset, Bourne, MA) spaced at 1 m intervals from the surface down to the bottom (20 m) and recorded the temperature every 5 minutes. These thermistors had an accuracy of 0.2 °C, a resolution of 0.02 °C and a response time of 5 minutes. The inshore site was located at 7 m depth, i.e. slightly above the mean depth of the thermocline. The site had a shallow slope of 1% and was instrumented with fast response thermistors (RBR Ltd, Ottawa, Ontario) having an accuracy of at least 0.005 °C, a resolution of  $5 \times 10^{-5}$  °C and a response time of less than 3 s. Four of these thermistors were attached to a vertical pole and deployed at 0.3, 0.6, 0.9, and 1.2 m above the sediments in 7 m of water. The temperature was recorded every 4 s. The temporal drift over the 31-day deployment was at most 8 s so no adjustment was made to the timing recorded by the thermistor units. A 3 beam, 1.5 MHz Acoustic Doppler Profiler (SonTek, San Diego, CA) was deployed on an A-frame facing downwards at the inshore site. This instrument was able to measure the velocity in the bottom 60 cm of the 7 m water column (from 1.5 cm above the sediments). The cell size was 3.1 cm with a blanking distance of 5 cm. Burst mode was used so that 24 profiles were collected every other minute. For the purposes of this research five of these 1 minute bursts were averaged to leave a data set with a 10 minute resolution.

The eastern, predominately downwind end of the South Arm basin of Lake Opeongo is covered with large rocks and boulders down to about 5–6 m. A fine layer of sediments settles on these boulders (Finlay *et al.* 2001; McCabe & Cyr 2006). At depths greater than 5 m, soft substrates are dominant. More sheltered subsections of the eastern shoreline are characterised by deep sandy substrates below 1 m depth. The western end of the basin is predominately upwind of the prevailing winds and is therefore generally more sheltered compared to the eastern end. The substrate in the west is typically coarse sand and small rocks down to 0.9 m with a soft substrate of sand mixed with mud covering the bedrock below about 1 m (Finlay *et al.* 2001; McCabe & Cyr 2006). Below 7–8 m, the lake sediment is dominated by gyttja, and the sedimentation is not influenced by surface

waves except during large storms in the fall (Finlay *et al.* 2001; McCabe & Cyr 2006).

Nitrogen and phosphorus are both available in the sediments or pore water of lakes (Søndergaard *et al.* 2001; Kirillin *et al.* 2009). The potential for phosphorus release during sediment resuspension events in near-shore areas of Lake Opeongo was shown by Cyr *et al.* (2009). Given the oligotrophic nature of Lake Opeongo, any nutrients that are released from the sediments (via any method) will contribute to the available food source for phytoplankton. The differences in substrate among different near-shore regions of Lake Opeongo (mud – coarse sands – boulders covered with fine sediments) may mean the ratio of nitrogen to phosphorus released from pore waters will differ among regions (McCabe & Cyr 2006; Cyr *et al.* 2009).

The distance a parcel of water is advected away from the boundary can be estimated if the benthic velocity field is known. The excursion length during a given time period,  $\Delta t$ , is equal to the average velocity over that time period multiplied by the time period,

$$L_{\Delta t} = \bar{u} \times \Delta t \quad (1)$$

Since the current over  $\Delta t$  may be changing magnitude as well as direction we use circular statistics to find the average velocity,  $\bar{u}$  over any period,  $\Delta t$ . The summation of the excursion lengths of individual time periods (Equation (1)) will be equal to the integral of the velocity over time,

$$L_x(t) = \int_{t_s}^{t_f} u \, dt, \quad L_y(t) = \int_{t_s}^{t_f} v \, dt, \quad (2)$$

where  $u$  and  $v$  are the speeds in the  $x$  and  $y$  directions, respectively,  $t_s$  is the initial time (July 15 in our case) and  $t_f$  is the final time (August 15). To calculate Equation (2) we first depth average the velocity data then calculate a running 10 minute temporal average of the velocity field. From this smoothed data the  $u$  and  $v$  components are taken to be along the vectors parallel and perpendicular to the major South Arm basin fetch, i.e. at 100° and 190° from  $N$ . Therefore  $L(t)_{\text{off}}$  is the average advection directed offshore, and  $L(t)_{\text{long}}$  is the advection directed alongshore. We are neglecting vertical velocities in our estimates of advection lengths,

as the observed vertical velocities are generally close to the detection limit of our Acoustic Doppler Profiler. These estimates of the Lagrangian particle excursion lengths  $L(t)$  are based upon Eulerian measurements, so do not follow a particular 60 cm deep benthic packet of water from the inshore site out into the pelagic region of South Arm as the horizontal velocity field is not uniform throughout the lake. Rather the particle excursion measure,  $L(t)_{\text{off}}$  gives us an idea of the potential for water transport originating from this inshore benthic region. If anything,  $L(t)$  is likely to be an underestimate of the advection scale of these water masses as the horizontal velocities induced by a basin scale seiche increase in the offshore direction. For example in a simple rectangular basin, the first horizontal mode wave has a sinusoidal form with the horizontal velocity maximum in the middle of the lake (Fricker & Nepf 2000).

## RESULTS

The benthic currents are correlated to changes in the stratification caused by upwelling or downwelling events at the western end of Lake Opeongo. Figure 3 (over two panels) shows the series of field data collected for this research. Figure 3(a) is the current speed while Figure 3(b) shows the direction of this current. Figure 3(c) shows a selection of isotherms calculated from the thermistor string at the offshore site and Figure 3(d) shows the temperatures from the four thermistors situated at the inshore site. Isotherms could not reasonably be calculated at the inshore site because there was not enough vertical resolution of temperature data. The current is greater than  $6 \text{ cm s}^{-1}$  on several occasions and in all of these occurrences the current direction is easterly, that is, flowing down the slope from the inshore site, directly along the South Arm major axis. In contrast the current upslope or inshore at this site is not as large or obvious, never going above  $6 \text{ cm s}^{-1}$  and never occurring in a similar upslope direction of any significant length of time. A current rose is shown in Figure 4(a), where it can be clearly seen that the strongest currents ( $>6 \text{ cm s}^{-1}$ ) are always directed in the offshore direction, i.e. the downslope currents are faster than the upslope currents. The overall water motions that are presented in Figure 3 are typical

for Lake Opeongo. Specifically we see periodic excursions of the thermocline offshore (Figure 3(c)) which are due to surface wind forcing inducing the basin scale seiche (Coman & Wells 2012). In 2009 the basin scale seiche period for the South Arm was measured to be 12 hours and the offshore isotherm data from this study confirm this measurement for this data set (Coman & Wells 2012). The offshore site is located closer to the western shore than the eastern shore of South Arm (see Figure 2) therefore we expect that when the offshore isotherms are decreasing in depth (i.e. moving closer to the surface) the temperature measured at the inshore thermistors will be decreasing due to the thermocline tilting inducing upwelling of the hypolimnion water at the western shore. This behaviour is confirmed by our data, particularly easy to observe during days 197–201, 202–204, 205–211 and 215–220. For the two extended ‘quiet’ periods (days 212–215 and 220–224) we measure weak winds (less than  $3 \text{ m s}^{-1}$ ) so that small surface forcing occurred during both these periods. The stratification at the benthic site is quite variable. At numerous times, the temperatures measured at the four thermistors are nearly uniform (Figure 3(d)) indicating that weak stratification exists at the inshore site, however there are also notable times of stronger stratification, for example day 201 and day 205. During these 2 days, the inshore water column becomes more stratified than at any other time in the record (up to  $4\text{--}5^\circ\text{C}$  over 90 cm compared to  $0.2\text{--}1.5^\circ\text{C}$  normally), suggesting that the highly stratified thermocline is intersecting the lakebed at the inshore measurement location at 7 m depth. Accompanying these times of inshore stratification are fairly smooth offshore isotherms and predominately southerly currents at the inshore site with magnitudes from 0 to  $3.5 \text{ cm s}^{-1}$ . A southerly current runs perpendicular to the major South Arm axis and parallel with the bathymetry at that site (Figure 2).

The distribution of horizontal currents at the inshore site is asymmetric, with the strongest currents ( $>6 \text{ cm s}^{-1}$ ) being directed offshore (Figure 4(a)). An estimate of the advection distances this implies can be found by calculating the total excursion lengths of the instantaneous advection for  $10^\circ$  bins over the entire sampling period (i.e.  $\Sigma L_{\Delta t}$ ). It should be emphasised that this is not a true Lagrangian estimate of a water parcel

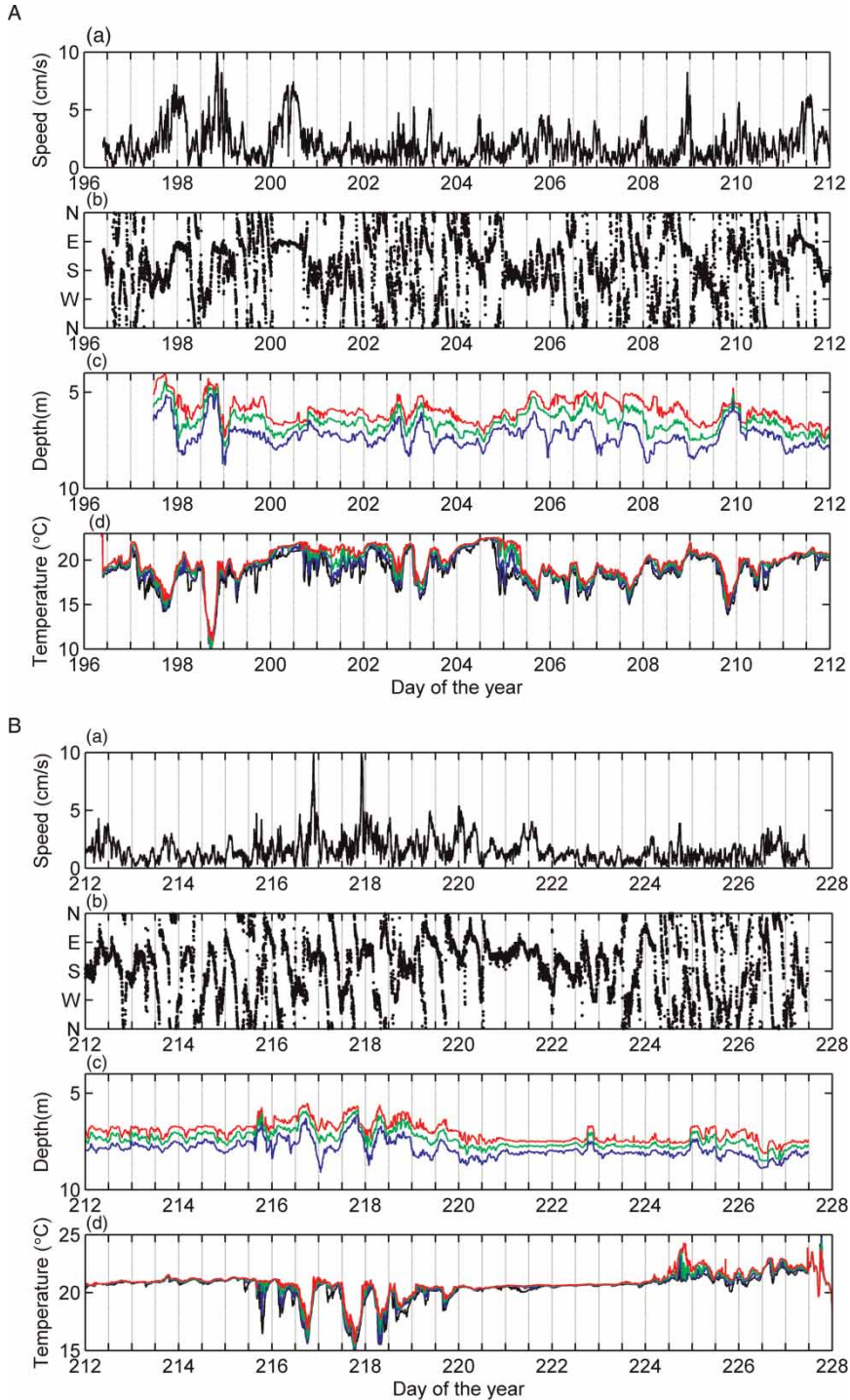


**Figure 3** | (a) Current speed at the inshore site, (b) current direction at the inshore site, (c) isotherms at the offshore site with the 15.5 °C isotherm in blue, 17.5 °C in green and 19 °C in red, and (d) isodepths (temperature at a fixed depth) at the inshore site, 0.3 m (black), 0.6 m (blue), 0.9 m (green) and 1.2 m (red) above the sediment. The full colour version of this figure can be found online at <http://www.iwaponline.com/wqrj/toc.htm>.

trajectory, but gives an idea of the magnitude of exchange potential of water parcels in each direction. We see that

$\Sigma L_{\Delta t}$  for the bins between 90 and 110° N is about four times that in any other direction. This range of peak

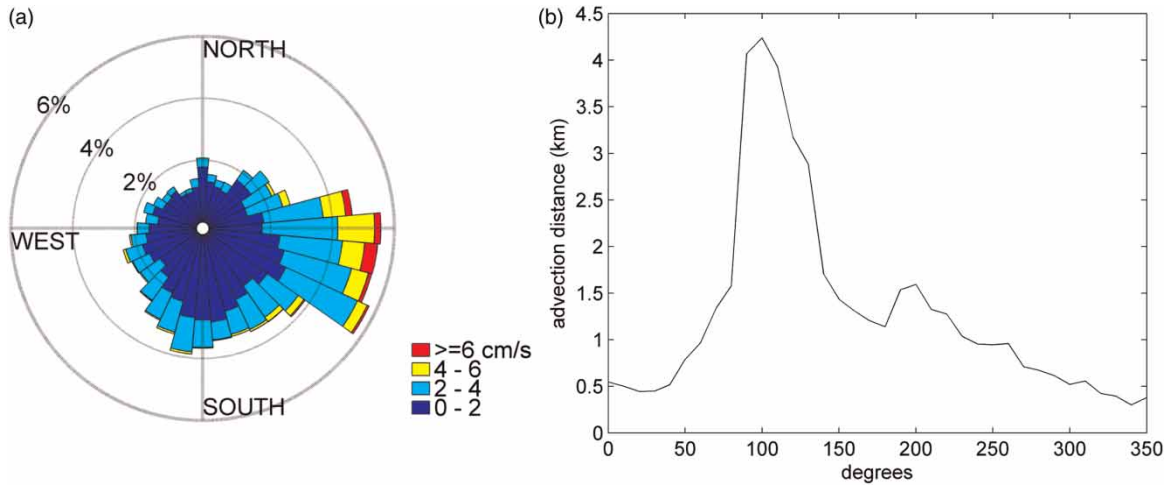


**Figure 4** | (a) A current rose showing the direction of benthic currents. (b) Total advection distance (km) over the 31-day deployment period as a function of direction at the inshore site. North is 0°.

excursion length covers the axis of South Arm basin which runs along 100° N. The second peak in this figure occurs around 200–210° N, which is almost perpendicular to the main transport direction and major South Arm axis. We now calculate the summation of the transport,  $L(t)$ , using the offshore and alongshore velocity projected onto the axis at 100° N and 190° N, respectively (see Figure 4(b)). Consistent with the current rose shown in Figure 4(a), the peaks greater than  $6 \text{ cm s}^{-1}$  in the offshore velocity time series and the corresponding velocity oscillations about 0 in the alongshore velocity time series simply show that the current is predominately offshore during these faster currents. The excursion length,  $L(t)$ , therefore quickly increases positively (i.e. advection offshore) during the periods of fast offshore benthic currents. At the end of the sampling period the total Lagrangian advection distance  $L(t)$  (as estimated from the Eulerian velocity data) reaches 16 km in the offshore direction and  $-10 \text{ km}$  in the alongshore direction (i.e. southerly). It is noteworthy that the overall transport is in the offshore direction so that on average water is moved from the inshore region into the pelagic waters of the lake. There are shorter periods when the transport is alternately inshore then offshore, so that the overall change in  $L(t)_{\text{off}}$  is minimal, for example days 201–202. Similarly, there is an overall transport of water in a southerly direction with periods of north–south equal distribution (days 199–201, 202–204 and 223–227) occurring between periods of southerly transport. The temporal

changes in offshore transport in Figure 5 shows the strong potential for offshore transport of benthic waters from the inshore site to extensive distances of South Arm basin. A single faster ( $>6 \text{ cm s}^{-1}$ ) current event can move benthic water from between 1.5 km over half a day (see day 197.5) to 2 km over an entire day (see day 200) with no balancing return of fluid at that depth. Circular statistics were used to calculate the average transport and the direction of this transport each day (noon–noon, see Figure 6).

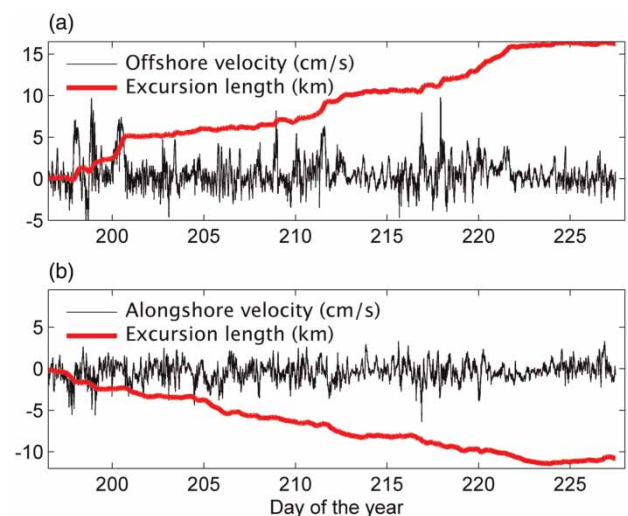


**Figure 5** | Velocity (black) and excursion length,  $L(t)$  (red) at the inshore site. In (a) velocity and excursion are positive in the east direction, in (b) velocity and excursion length are positive in the north direction. The y-axis in each subfigure is 21.5 units of either velocity in  $\text{cm s}^{-1}$ , or distance in km. The full colour version of this figure can be found online at <http://www.iwaponline.com/wqrj/toc.htm>.

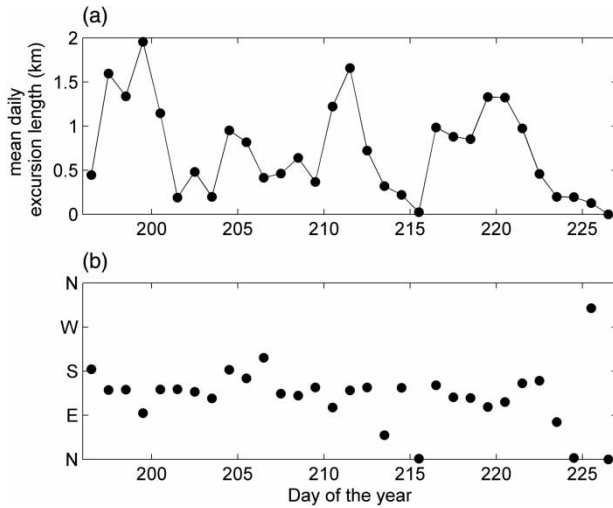


**Figure 6** | (a) Mean daily excursion length (km), and (b) the direction of excursion.

The maximum mean daily transport occurs for day 199.5–200.5 in an easterly (that is, offshore) direction, and had a value of 2 km. Over the deployment period, the average advection distance in a day was 630 m in a south east direction (134 N). There are only 5 days when the daily transport is not in the easterly to south easterly range and these all correspond to days when the transport is less than 250 m. The normalised histogram of current speeds from the inshore site (Figure 7) highlights the small percentage of time that the faster currents exist for

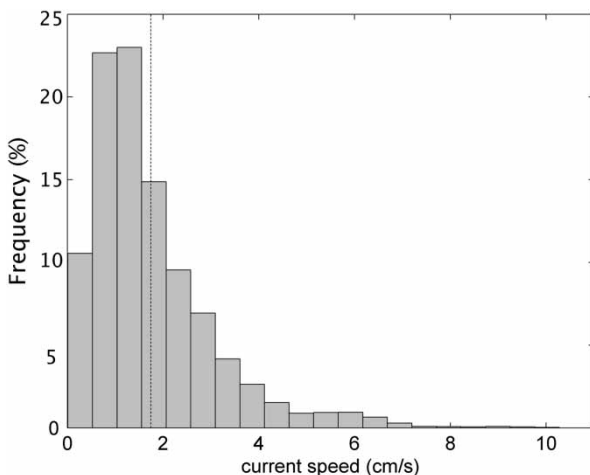


**Figure 7** | Normalised histogram of current speeds from the inshore site over the deployment period. These speeds are 1 minute averages from the 60 cm range above the sediment. The mean current speed of  $1.75 \text{ cm s}^{-1}$  is shown as the vertical dashed line.

(currents  $>6 \text{ cm s}^{-1}$  occur for 4% of the time). The arithmetic mean current speed of  $1.75 \text{ cm s}^{-1}$  is shown on this plot.

## DISCUSSION

Most of the changes in temperature, velocity and stratification at the inshore site are consistent with the movements of the thermocline resulting from a basin scale seiche period of 12 hours (as reported in Coman & Wells 2012). A new observation is that the magnitude of the benthic offshore currents is greater than the benthic onshore currents. Rather than a simple oscillation up and down the slope, there is a net offshore transport of water from the benthic inshore region of the lake. This observation warrants further study to determine whether there is either an asymmetry between the upslope and downslope flows (Nakayama & Imberger 2010), or whether the net offshore transport is part of a larger basin scale flow whereby on average water is drawn in at the edges of the lake and exits in the central axis of the lake.

The velocity exceeded  $6 \text{ cm s}^{-1}$  on seven occasions during the record, which were all accompanied by larger offshore excursion lengths in the positive offshore direction. Four of these were clearly associated with the recession of an upwelling at the western inshore site (day 198, 199, 217 and 218) while the other three (day 200, 209 and 211) are associated with a downwelling event in the west, driven by easterly winds (Figure 3). Given the depth of our inshore site (7 m) and the depth of the thermocline (7–9 m), an upwelling event is easily observed in a plot of temperatures measured at the inshore site (Figure 3(d)) because the difference between a non-seiching 7 m depth temperature (about 19–21 °C) and hypolimnion temperatures (10–15 °C) is much larger than the temperature difference between non-seiching 7 m depth temperatures and a downwelling epilimnion (22–25 °C). However, close inspection of some offshore current data shows that surface currents on days 200, 209 and 211 are westerly and therefore driven by easterly winds and cause a downwelling at the western shore of South Arm basin. Consistent with the slight increase in isotherm depth at the inshore site and isotherm depth increases at the offshore site. Therefore, all of the faster

current events in our record occur when the inshore temperatures are increasing, that is, during the recession of an upwelling event (caused by westerly winds) or during the beginning of a downwelling event (caused by easterly winds).

The estimates of the large excursion lengths of the water parcels suggest that there should be strong exchange between the littoral and pelagic zones of Lake Opeongo. The measurements of strong unidirectional benthic currents that last for hours (rather than minutes) gives rise to the potential for substantive offshore water transport in Lake Opeongo rather than localised transport contained to the inshore region due to evenly oscillating currents. The depth at which water transported from the inshore region will enter the larger lake basin will depend upon the density of the mixed inshore benthic water and of the stratification offshore. The downslope and faster currents typically occur as the upper portion of the thermocline is moving down the slope. During the sampling period the thermocline was located close to the 15 °C isotherm at depths between 7 and 10 m. Hence water from the littoral zone that is potentially nutrient rich, will enter the pelagic waters of Lake Opeongo in the upper thermocline, where it may subsequently be available for primary production.

The speeds reached during the large downslope currents were often greater than 6 cm s<sup>-1</sup> so are large enough at the inshore site to draw pore water and associated nutrients out of the sediments (Gloor *et al.* 1994). Sediment resuspension is another possible mechanism to bring nutrients into the water column, but this requires high near bed velocities. For example, our mean (1.75 cm s<sup>-1</sup>) and maximum current (10.3 cm s<sup>-1</sup>) velocities near the lake bed are very similar to those measured by Gloor *et al.* (1994), where the root mean square of the bottom current speed was 2 cm s<sup>-1</sup> and burst speeds were of the order of 7 cm s<sup>-1</sup>. For these velocities, Gloor *et al.* (1994) concluded that the mean speeds would not lead to sediment resuspension, but that it was possible for the highest near bed velocities. Velocities exceeding 7 cm s<sup>-1</sup> only occur in 0.7% of our record, and generally occurred after large seiches. The substrate at the inshore site is fine mud/silt and due to the cohesive nature of this sediment, direct resuspension will be difficult given the mean current speeds. Surface water waves are able to resuspend sediments in the shallow littoral zone of Lake

Opeongo (Cyr *et al.* 2009). If similar sized currents occur within the 1–5 m depth range as occurs at 7 m depth then nutrients resuspended via surface waves may also be transported offshore, perhaps at shallower depths given the warmer temperatures that will be present at sites further inshore of our inshore site.

## CONCLUSIONS

In Lake Opeongo, the wind-driven internal seiche drives benthic velocities in the near-shore regions that are on average 1.75 cm s<sup>-1</sup>, with brief periods where the maximum current is up to 10 cm s<sup>-1</sup>. The current is greater than 6 cm s<sup>-1</sup> on several occasions and in all of these occurrences the current direction is offshore, that is, flowing down the slope. In general we find that the downslope currents are faster than the upslope currents at our inshore site, located at the upwind end of South Arm basin. Near bed velocities greater than 6 cm s<sup>-1</sup>, occur only 4% of the time, suggesting that there is infrequent potential for sediment resuspension. The maximum mean daily transport occurs for day 199.5–200.5 in an easterly (that is, offshore) direction, and had a value of 2 km per day. The average daily mean transport over the deployment period is 630 m in a south east direction (134 N).

Transport of bottom water occurs most strongly in the offshore direction when isotherm motions due to thermocline deflection are largest. Calm periods show either an equal onshore/offshore transport or a small net offshore transport. While the mean currents are unlikely to resuspend any sediment, they can result in daily advection of water of 0.6 km. As the South Arm of Lake Opeongo has a length of 6 km and a mean width of 0.6 km, the advection by the mean current means that the water at the depth of the thermocline in the near-shore zone is able to exchange with the pelagic waters. This constant exchange has implications for the nutrient cycling in the water column, and suggests that near-shore and offshore sites are well connected, particularly after large seiching events.

We found that the near bed velocity at 7 m depth was greatest after strong seiche events, and on average was directed offshore. Such an asymmetry in the near bed velocity could be due to processes associated with boundary

mixing described by Nakayama & Imberger (2010), or could indicate a more complicated 3D circulation pattern in the lake in response to wind-driven forcing. The velocity exceeded  $6 \text{ cm s}^{-1}$  about 4% of the time. This occurred during seven strong events (day 198, 199, 200, 209, 211, 217 and 218), which were all associated with corresponding seiche driven offshore isotherm and inshore temperature movements. We expect these events in particular increased nutrient addition to the benthic boundary layer through advection of pore water and possibly occasional (<0.7% of the time) sediment resuspension given speeds  $>7 \text{ cm s}^{-1}$  that were occasionally reached (Gloor *et al.* 1994). The mean current speed is expected to enable pore water advection along the mean excursion length, which can still connect the near-shore and offshore regions at the depth of the thermocline. Therefore any nutrients pumped into the water column have the potential to be transported far offshore under strong wind conditions or at least into the pelagic zone under mean wind conditions. Given that Lake Opeongo is oligotrophic, nutrients are likely absorbed quickly by local plankton which themselves can then be transported into the pelagic zone to become available as food to other trophic levels.

## ACKNOWLEDGEMENTS

The fieldwork was made possible by support from Mark Ridgeway and the OMNR Harkness field station. Coman was supported by a Post Doctoral Fellowship from the University of Toronto's Centre of Global Change Science. Wells received funding from the Natural Sciences and Engineering Research Council of Canada, the Canadian Foundation for Innovation and the Ontario Ministry of Research and Innovation.

## REFERENCES

- Basterretxea, G., Jordi, A., Garcés, E., Anglès, S. & Reñé, A. 2011 Seiches stimulate transient biogeochemical changes in a microtidal coastal ecosystem. *Mar. Ecol. Prog. Ser.* **423**, 15–28.
- Coman, M. A. & Wells, M. G. 2012 Temperature variability in the near-shore benthic boundary layer of Lake Opeongo is due to wind driven upwelling events. *Can. J. Fish. Aquat. Sci.* **69**, 282–296.
- Cyr, H., McCabe, S. K. & Nürnberg, G. K. 2009 Phosphorus sorption experiments and the potential for internal phosphorus loading in littoral areas of a stratified lake. *Water Res.* **43**, 1654–1666.
- Finlay, K., Cyr, H. & Shuter, B. J. 2001 Spatial and temporal variability in water temperatures in the littoral zone of a multibasin lake. *Can. J. Fish. Aquat. Sci.* **58**, 609–619.
- Fricker, P. & Nepf, H. 2000 Bathymetry, stratification and internal seiche structure. *J. Geophys. Res.* **105** (C6), 14237–14251.
- Gloor, M., Wüest, A. & Münnich, M. 1994 Benthic boundary mixing and resuspension induced by internal seiches. *Hydrobiologia* **284**, 59–68.
- Hawley, N. & Muzzi, R. W. 2003 Observations of nepheloid layers made with an autonomous vertical profiler. *J. Great Lakes Res.* **29**, 124–133.
- Horn, D. A., Imberger, J. & Ivey, G. N. 2001 The degeneration of large-scale interfacial gravity waves in lakes. *J. Fluid Mech.* **434**, 181–207.
- Imberger, J. & Patterson, J. 1990 Physical Limnology. *Adv. Appl. Mech.* **27**, 303–473.
- Inall, M. E. 2009 Internal wave induced dispersion and mixing on a sloping boundary. *Geophys. Res. Lett.* **36**, L05604.
- King, J., Shuter, B. & Zimmerman, A. 1999 Signals of climate trends and extreme events in the thermal stratification pattern of multibasin Lake Opeongo, Ontario. *Can. J. Fish. Aquat. Sci.* **56**, 847–852.
- Kirillin, G., Engelhardt, C. & Golosov, S. 2009 Transient convection in upper lake sediments produced by internal seiching. *Geophys. Res. Lett.* **36**, L18601.
- Levine, S. N. & Schindler, D. W. 1992 Modification of the N:P ratio in lakes by *in situ* processes. *Limnol. Oceanogr.* **37**, 917–935.
- Lorke, A. 2007 Boundary mixing in the thermocline of a large lake. *J. Geophys. Res.* **112**, C09019.
- MacIntyre, S., Flynn, K. M., Jellison, R. & Romero, J. R. 1999 Boundary mixing and nutrient fluxes in Mono Lake, California. *Limnol. Oceanogr.* **44**, 512–529.
- McCabe, S. K. & Cyr, H. 2006 Environmental variability influences the structure of benthic algal communities in an oligotrophic lake. *Oikos* **115**, 197–206.
- Michallet, H. & Ivey, G. N. 1999 Experiments on mixing due to internal solitary waves breaking on uniform slopes. *J. Geophys. Res.* **104**, 13467–13477.
- Nakayama, K. & Imberger, J. 2010 Residual circulation due to internal waves shoaling on a slope. *Limnol. Oceanogr.* **55**, 1009–1023.
- Ostrovsky, I., Yacobi, Y. Z., Walline, P. & Kalikhman, I. 1996 Seiche-induced mixing: its impact on lake productivity. *Limnol. Oceanogr.* **41**, 323–332.
- Rao, D. B. & Murty, T. S. 1970 Calculation of the steady state wind-driven circulations in Lake Ontario. *Arch. Meteorol. Geophys. Bioklimatol. A.* **19**, 195–210.

- Read, J. S., Hamilton, D. P., Jones, I. D., Muraoka, K., Winslow, L. A., Kroiss, R., Wu, C. H. & Gaiser, E. 2011 [Derivation of lake mixing and stratification indices from high-resolution lake buoy data](#). *Environ. Model. Softw.* **26**, 1325–1336.
- Shteinman, B., Eckert, W., Kaganowsky, S. & Zohary, T. 1997 Seiche-induced resuspension in Lake Kinneret: a fluorescent tracer experiment. *Water, Air Soil. Pollut.* **99**, 123–131.
- Søndergaard, M., Jensen, P. J. & Jeppesen, E. 2001 [Retention and internal loading of phosphorus in shallow, eutrophic lakes](#). *Sci. World J.* **1**, 427–442.
- Stevens, C. L. & Lawrence, G. A. 1997 [Estimation of wind-forced internal seiche amplitudes in lakes and reservoirs, with data from British Columbia, Canada](#). *Aquat. Sci.* **59**, 115–134.
- Sundbäck, K., Miles, A., Hulth, S., Pihl, L., Engström, P., Selander, E. & Svenson, A. 2003 [Importance of benthic nutrient regeneration during initiation of macroalgal blooms in shallow bays](#). *Mar. Ecol. Progress Ser.* **246**, 115–126.
- Wain, D. J. & Rehmann, C. R. 2010 [Transport by an intrusion generated by boundary mixing in a lake](#). *Water Resour. Res.* **46**, W08517.
- Wells, M. G. & Parker, S. 2010 [The thermal variability of the waters of Fathom Five National Marine Park, Lake Huron](#). *J. Great Lakes Res.* **36**, 570–576.

First received 5 December 2011; accepted in revised form 18 July 2012